applied sciences

MDPI

Article

A High-Resolution Ultrasonic Ranging System Using Laser Sensing and a Cross-Correlation Method

Lecheng Jia [1,†], Bin Xue [2,†], Shili Chen [1,*], Hanzhong Wu [2], Xiaoxia Yang [3], Jingsheng Zhai [2,*] and Zhoumo Zeng [1]

1 State Key Laboratory of Precision Measurement Technology and Instrument, Tianjin University, Tianjin 300072, China; jialecheng@tju.edu.cn (L.J.); zhmzeng@tju.edu.cn (Z.Z.)
2 School of Marine Science and Technology, Tianjin University, Tianjin 300072, China; xuebin@tju.edu.cn (B.X.); wuhz@tju.edu.cn (H.W.)
3 Tianjin Key Laboratory of Information Sensing and Intelligent Control, Tianjin University of Technology and Education, Tianjin 300222, China; yangxiaoxia0925@163.com
* Correspondence: slchen@tju.edu.cn (S.C.); jingsheng@tju.edu.cn (J.Z.); Tel: +86-22-2740-2366 (S.C.)
† These authors contributed equally to this work.

Received: 4 March 2019; Accepted: 8 April 2019; Published: 9 April 2019

check for updates

Abstract: Ultrasound has been proven to be a valid tool for ranging, especially in water. In this paper, we design a high-resolution ultrasonic ranging system that uses a thin laser beam as an ultrasonic sensor. The laser sensing provides a noncontact method for ultrasound detection based on acousto-optic diffraction. Unlike conventional methods, the ultrasound transmitted from the transducer is recorded as the reference signal when it first passes through the laser. It can be used to improve the accuracy and resolution of the time-of-flight (TOF) by a cross-correlation method. Transducers with a central frequency of 1 MHz and diameters of 20 mm and 28 mm are used in the experiment. Five targets and a test piece are used to evaluate the ranging performance. The sound velocity is measured by the sound velocity profiler (SVP). The repeatability error of TOF is less than 4 ns, and the theoretical resolution of TOF is 0.4 ns. The results show a measurement resolution within one-tenth of the wavelength of ultrasound and an accuracy better than 0.3 mm for targets at a distance up to 0.8 m. The proposed system has potential applications in underwater ranging and thickness detection.

Keywords: Laser sensing; ultrasonic ranging; acousto-optic effect; cross-correlation

1. Introduction

Ultrasonic pulse-echo detection dates from 1912, where it was used for iceberg detection. The basis of pulse-echo detection is echolocation. The distance between the transducer and the object depends on the TOF of the ultrasonic pulses [1]. The shape of the object can be reconstructed using a scanning imaging system or an array of transducers [2,3].

Compared to other detection methods (radar or laser), ultrasound is more suitable in water [4,5]. On one hand, the reflection coefficient of an interface depends on the mismatch in acoustic impedance of the materials on either side of the interface. The objects to be measured are usually placed in water to allow sufficient energy transfer from and into the transducer, which is called immersion ultrasound detection [6]. On the other hand, sound is a valid method for underwater detection, especially in the deep ocean because of the high attenuation of electromagnetic waves in water. Currently, ultrasonic pulse-echo detection has been widely used in thickness detection, ranging, single/multi beam echo sounding, and sonar [7–10].

There are two main types of ultrasonic ranging methods. One is the pulse-echo type [11], and the other is the opposite type [12]. The pulse-echo type consists of only one transducer, which works in transmit–receive mode. The transducer emits a short ultrasonic pulse. It is reflected by the target. Then the echo is received by the same transducer. The opposite type usually consists of two transducers; one works in transmit mode and the other works in receive mode. The transmitting transducer emits a short ultrasonic pulse. Then, the pulse is received by the receiving transducer, which is attached to the target. One of the distance measurement methods is the phase shift method. It evaluates distance by computing the phase difference between transmitted and received continuous waves, overcoming traditional acoustic attenuation problems [13]. A multiple-frequency continuous wave is used to improve the ranging accuracy in phase shift method [14]. However, it requires a continuous wave and works in the opposite type only.

For ranging or thickness detection, the pulse-echo type is more suitable. It is common to measure the time-of-flight (TOF) to determine the distance [15]. In this case, the TOF is the time that a transmitted pulse takes to reflect back to the receiver. We can calculate the distance in cases where the sound velocity is known. One of the conventional methods for determining the TOF is the threshold method [16]. This method is simple and fast. The TOF is determined when the received signal first exceeds a given threshold level. Curve-fitting is another method for TOF calculation [17]. It accurately estimates the shape factors of the echo envelope, as well as locates its onset. It is possible to assure reduced bias and uncertainty in critical TOF measurements. A more suitable TOF estimation technique is cross-correlation [18–20]. Here, the transmitted and received signals are cross-correlated. The time at which the correlation result reaches its maximum is an estimation of the TOF. In recent years, it has been used in absolute distance measurement in laser ranging [21,22]. Methods with similar theoretical bases are also used in ultrasonic ranging and thickness detection [23,24]. Cross-correlation methods are helpful for improving the accuracy and resolution to the phase level.

However, the reference signal is difficult to record due to the drawbacks associated with the conventional piezoelectric transducer [25]. For example, there is much noise in the initial pulse when the transducer works in transmit–receive mode. It is not suitable to be the reference signal to calculate the TOF. Compared to piezoelectric transducer, a laser beam can be a good sensor to receive ultrasound with no interference from the sound field, which is based on the acousto-optic effect. Acousto-optics has been widely used to make tunable optical filters, modulators, and Q-switches [26–30]. Research focused on quantitative analyses for ultrasound that uses acousto-optic diffraction began with Raman and Nath [31] in 1936. Klein and Cook [32] proposed the criterion for the Raman–Nath diffraction regime. Abeele [33] made analytical and numerical solutions for the extended Raman–Nath equations when the light was diffracted by ultrasonic pulses. With the development of these theories, some optical detection methods have been proposed. The Schlieren method is one of the optical detection methods used for visualizing sound fields [34–36]. It offers high measurement speeds for visualizing entire acoustic fields in real time, without disturbing the ultrasound fields. In addition, light diffraction tomography makes it possible for the noncontact detection of the characterizations of ultrasound, such as sound pressure, phase, and ultrasonic power [37,38]. It is also suitable for air-coupled transducers [39]. However, all studies are aimed at characterization of ultrasound and sound field visualization. The acousto-optic effect would have great potential if used in ultrasonic ranging.

The aim of this work is to show that the optical detection for ultrasound based on acousto-optic diffraction is helpful for improving the ultrasonic ranging resolution. The ultrasound transmitted from a transducer is referred to as a reference signal when it first passes through the laser beam. When the echo passes through the laser again, it generates another signal, carrying the distance information. As the optical detection is a noncontact detection, the reference signal is stable and clean compared to conventional methods. A cross-correlation method is used to determine the time interval between the reference signal and echoes, which directly reflects the distance between the laser beam and the surface of the target. This paper is organized as follows: The principles of acousto-optic diffraction and the pulse-echo ultrasonic ranging method are introduced first. Then, a pulse-echo ultrasonic ranging method based on a laser sensing system is established. The TOF according to the cross-correlation method, sound velocity, and ranging resolution is discussed. Ranging results of five targets are compared with the coordinate measuring machine. An aluminum test piece is used to evaluate the thickness detection results compared to the micrometer. The ranging uncertainty of the proposed system is discussed at the end of the document.

2. Theory

2.1. Acousto-Optic Diffraction

In this section, we describe the relationship between the continuum mechanics of ultrasound and the optical diffraction problem. Ultrasonic waves can be seen as a kind of mechanical wave. In an isotropic medium, such as water, the index of refraction changes with pressure, which is induced by the ultrasound. The relationship between the refractive index and density of the medium can be written as follows:

$$n(\mathbf{r},t) = \sqrt{1+\chi\rho(\mathbf{r},t)/\rho_0}, \tag{1}$$

where $n(\mathbf{r},t)$ is the refractive index of the medium at location $\mathbf{r}$ at time t, $\rho(\mathbf{r},t)$ is the corresponding material density, χ is the intrinsic susceptibility of the medium, and ρ_0 is the ambient density of the medium. Using Taylor series expansion algebraic transformation, Equation (1) can be written as follows:

$$n(\mathrm{r},t) = n_0 + \frac{n_0^2-1}{2\rho_0 n_0}[\rho(\mathrm{r},t)-\rho_0], \tag{2}$$

where n_0 represents the ambient refractive index. We assume that the sound pressure is small and that the density variation can be related to the pressure variation using the piezo-optic coefficient. As such, the relationship between the index of refraction and the sound pressure is directly proportional, as follows:

$$n(\mathrm{r},t) = n_0 + \frac{\partial n}{\partial p}p(\mathrm{r},t). \tag{3}$$

The $\partial n/\partial p$ is the piezo-optic coefficient, which can be expressed as follows:

$$\frac{\partial n}{\partial p} = \frac{n_0^2-1}{2n_0\rho_0 c_0^2}, \tag{4}$$

where c_0 is the sound velocity. Here, we establish the relationship between the sound pressure and the refractive index. The ultrasound can be a continuous wave or pulsing wave.

When a laser beam intersects the ultrasound field, it is diffracted and split into several beams that propagate in different directions. Raman and Nath [31] presented the analytical solution of acousto-optic diffraction, which was known as Raman–Nath diffraction. Pitts [36] explained the weak scattering model for the interaction of the optical and acoustic pulses in the Raman–Nath regime. The criterion for the Raman–Nath diffraction regime is defined by the Klein–Cook parameter Q [32] as follows:

$$Q = \frac{2\pi\lambda_L L}{n_0\lambda_S^2}, \tag{5}$$

where λ_L is the wavelength of light, λ_S is the wavelength of ultrasound, and L represents the length of the interaction volume. When $Q < 1$, Raman–Nath diffraction occurs.

When an ultrasonic pulse propagates through the medium, it modulates the amplitude and frequency of the laser. The mth order of diffracted light can be expressed as follows:

$$E_m = A\cdot J_m(\varphi(t))e^{i(\omega+m\Omega)t}, \tag{6}$$

where A is a constant, ω is the angular frequency of light, and Ω is the angular frequency of ultrasound. J_m is the Bessel function of the mth order. The frequency of the diffracted light corresponds to the frequency of the ultrasound and the diffracted order. The phase delay induced by the ultrasound $\varphi(t)$ can be expressed as follows:

$$\varphi(t) = k_L \frac{\partial n}{\partial p} \int_0^L p(y,t)dy, \tag{7}$$

where k_L is the wavenumber of the light, $\partial n/\partial p$ is the piezo-optic coefficient of the medium, and $p(y,t)$ is the pressure of ultrasound along the direction of light. The direction of light propagation is seen as the y-axis, which is the path of integration. The principle of acousto-optic diffraction is shown in Figure 1. At this point, we present the relationship between diffracted light and ultrasound. We can calculate an ultrasonic pulse through the diffracted light. As the width of laser beam is only 0.8 mm, it provides a noncontact and high spatial resolution means for ultrasound detection.

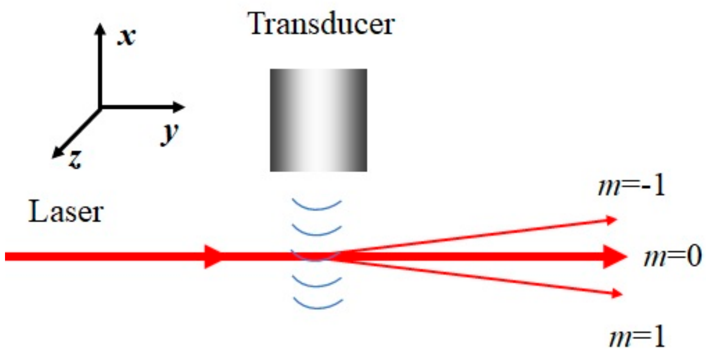

Figure 1. The principle of acousto-optic diffraction; m is the diffraction order.

2.2. Pulse-Echo Ultrasonic Ranging

As shown in Figure 2a, the pulse-echo ultrasonic ranging system is based on echo-location. The transducer and the test piece are in the water. The result of the pulse-echo signal is shown in Figure 2b. The initial pulses are generated by electrical noise and a piezoelectric signal. When the distance is not too long and the temperature is stable, the ultrasound is assumed to travel along a straight line. The position of the scatter is determined by the TOF of the echo wave. The envelope of the signal is calculated by the Hilbert transform (HT), which has been widely used in nonstationary signal analysis [40].

If we consider the pulse-echo signal as $x(t)$, the HT of $x(t)$ is defined as follows:

$$H[x(t)] = \pi^{-1} \int_{-\infty}^{+\infty} \frac{x(\tau)}{t-\tau} \mathrm{d}\tau. \tag{8}$$

The envelope of $x(t)$ is shown in Figure 2b. The peaks of the envelope determine the TOF. If the sound velocity is known, we can calculate the distance between the scatter and the transducer.

The range information depends on the TOF. The phase-based methods have higher resolution than amplitude-based methods. Cross-correlation is a measure of similarity of two series as a function of the displacement of one relative to the other [41]. It is used for searching a long signal for a shorter, known feature. For discrete functions, the cross-correlation is defined as follows:

$$(f * g)[n] = \frac{1}{N} \sum_{m=-\infty}^{\infty} f^*[m] g[m+n], \tag{9}$$

where f^* denotes the complex conjugate of f, N is the length of the series, and m ranges from 0 to $N-1$. Cross-correlation is useful for determining the time delay between two signals. After calculating the cross-correlation between the two signals, the maximum of the cross-correlation function indicates the point in time where the signals are best aligned. The time delay between the two signals is determined by the argument of the maximum. As opposed to other TOF methods, such as amplitude-related methods, cross-correlation methods need a reference signal. However, as shown in Figure 2b, there are many electronical noises in the initial ultrasound pulse when using the piezoelectric transducer. It is not suitable to be used as reference signal, which makes it difficult to determine the time of start.

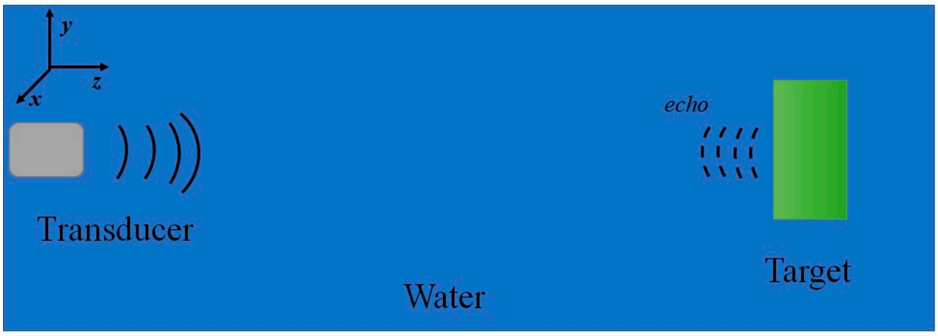

(a)

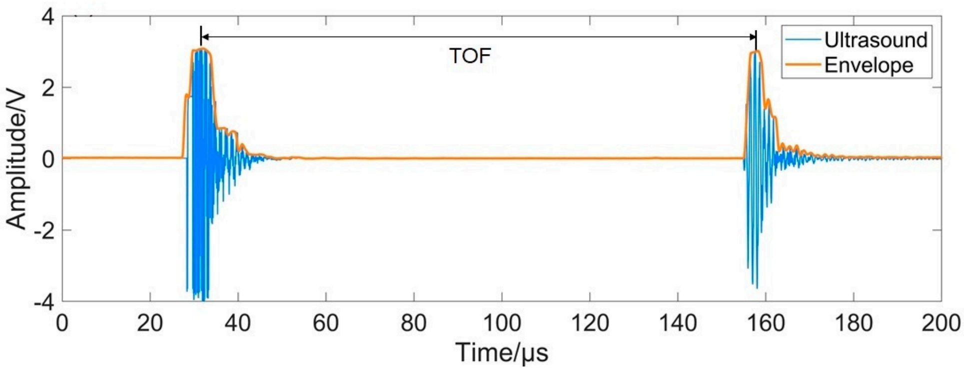

(b)

Figure 2. (**a**) Schematic of pulse-echo ultrasonic ranging; (**b**) a result of the pulse-echo signal and the time-of-flight (TOF).

As mentioned in Section 2.1, a laser beam can be used as a noncontact ultrasonic sensor. Therefore, we can use the signal when the ultrasonic pulse first propagates through the laser as the reference signal to calculate the TOF by the cross-correlation method. In the following sections, acousto-optic diffraction and the cross-correction method are used to improve the resolution and accuracy of ultrasonic ranging using the same ultrasonic transducer.

3. Experimental Set-Up

The pulse-echo ultrasonic ranging system is shown in Figure 3. The instruments used in the system are listed in Table 1.

Table 1. Instruments used in ranging system.

Instrument	Description
Signal generator	Tektronix AFG3000C
Amplifier	Homemade, amplification factor: 36 dB
He-Ne laser	Thorlabs, 633 nm, 5 mW
Photodetector	Thorlabs, APD430 A/M, 400 nm–1000nm
Digital oscilloscope	Tektronix MDO3104, maximum sample rate: 5 G/s, resolution: 8 bits
Transducer	Goworld, 1P20, 1 MHz, 20 mm
Transducer	Goworld, 1P28, 1 MHz, 28 mm, immersion
Displacement platform	Thorlabs, travel: 25 mm, engraving: 0.01 mm
Water tank	100 cm × 30 cm × 50 cm, glass
Sound velocity profiler (SVP)	Valeport Mini SVP, resolution: 0.001 m/s, uncertainty of sound velocity: 0.02 m/s

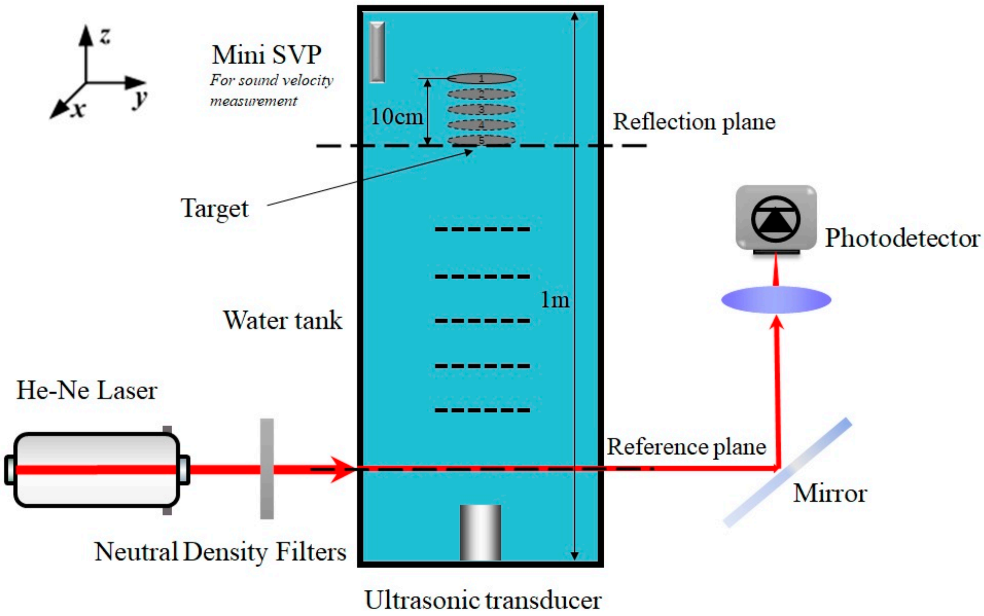

Figure 3. Pulse-echo ultrasonic ranging system.

The He-Ne laser emitted a continuous light into the water, assuming that the medium did not absorb it. The diffracted light was reflected by the mirror and was detected by the photodetector. Please note that diffracted light of high order ($m > 1$) was neglected in our experiment due to the low intensity. The positions of the transducer and the laser were fixed. A system with similar equipment has been used for the characterization of pulsed ultrasound; more details are provided in the original paper [42].

Both transducers were plane transducers with a central frequency of 1 MHz. The difference is that 1P28 is an immersion transducer with a 1/4 wavelength layer that is acoustically matched to water. The direction of ultrasound propagation is considered as the z-axis. Accordingly, the direction of the laser propagation is considered as the y-axis.

The sound velocity was measured by a commercial SVP (Valeport Mini SVP). The principle of sound velocity measurement was by a sing-around method. The TOF was measured by the time of multiple round trips of sound waves within a known distance.

There were five targets used in the experiment, as shown in Figure 4. The targets were mirrors whose diameters were 1 inch. All targets were fixed on the aluminum breadboard. The hole spacing was 25 mm. The transducer was fixed in the same line to ensure that the ultrasound propagated along the z-axis. We measured the distance between the reference plane and the reflectors. As the reflector could reflect ultrasound, we removed the reflectors one by one during the measurement, so that we could get the distance to the five reflectors one by one.

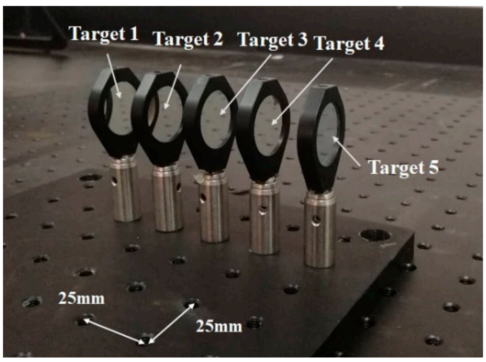

Figure 4. Targets used in the experiment.

4. Results

Two kinds of excitation signals, namely a sinusoidal burst signal and a pulse signal, were used to excite the transducer. The ultrasound signal was detected by the ultrasonic transducer and laser sensing system.

The pulse signal was a high voltage sharp pulse generated by the reflectoscope, which is shown in Figure 5a. In this situation, the transducer worked in transmit–receive mode. The ultrasonic signal is shown in Figure 5b. The details of the initial wave and echo wave are shown in Figure 5c,d. The width of the initial wave is quite wide and noisy. It is difficult to determine the time of start of the TOF. The laser sensing system provided a noncontact detection for ultrasound. Although the laser beam was placed near the surface of the transducer, the initial wave (also seen as a reference wave here) was cleaner and shorter than the ultrasonic transducer, which is shown in Figure 5f. However, the ultrasound emitted by the sharp pulse was generated by self-vibration of the piezoelectric materials. The stability and the signal-to-noise radio (SNR) were not good enough for precise measurement. The initial signal was also unsuitable for cross-correlation calculations.

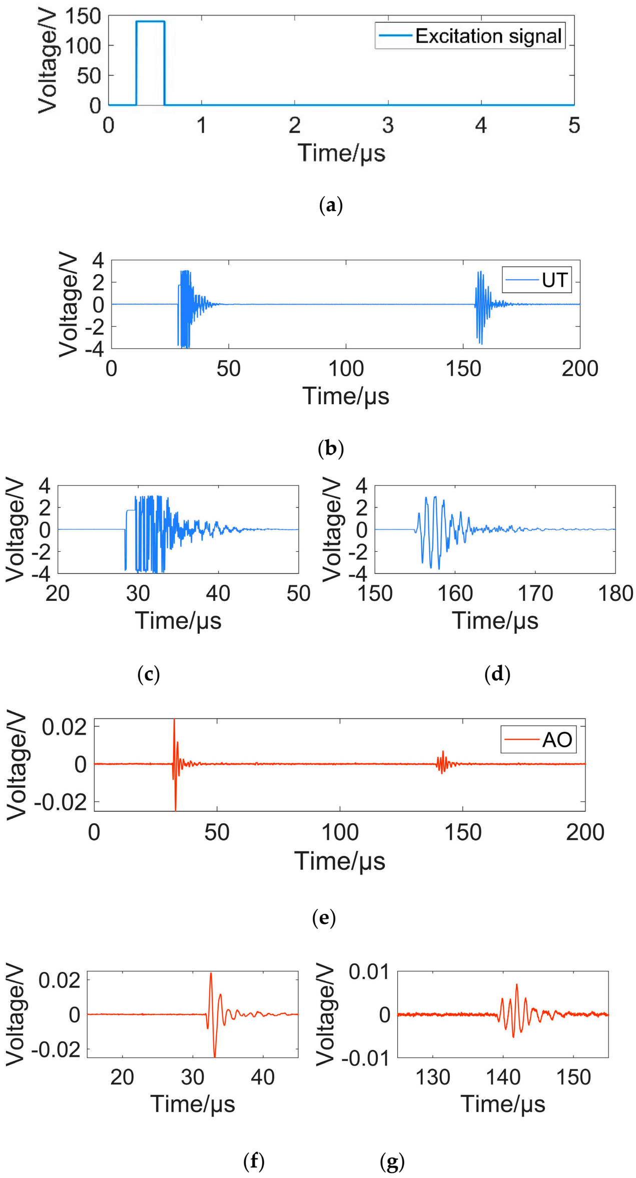

Figure 5. Ultrasound excited by pulse signal: (**a**) Pulse signal; (**b**) ultrasound signal detected by ultrasonic transducer; (**e**) ultrasound signal detected by laser sensing system; (**c**,**d**,**f**,**g**) zooms of the signal.

To transmit a stable and controllable ultrasonic signal, we instead used a sinusoidal burst signal. The sinusoidal burst signal was a 5-cycle 1 MHz burst signal generated by the signal generator, which is shown in Figure 6a. The transducer worked in transmit mode, which only transmits ultrasound. The laser sensing system was used for ultrasound detection. Figure 6b–d show the ultrasound signal detected by the laser sensing system. In this case, the ultrasound was generated by forced vibration. We clearly found 5-cycle rising pulses and several small vibrations in the initial and echoed wave.

The ultrasound excited by the sinusoidal burst signal was stable and controllable, and therefore could be a good reference signal for the cross-correlation method. The laser sensing system provided an ultrasound detection method without disturbing the ultrasound field. Therefore, the sinusoidal burst signal and laser sensing system were used in the following experiment.

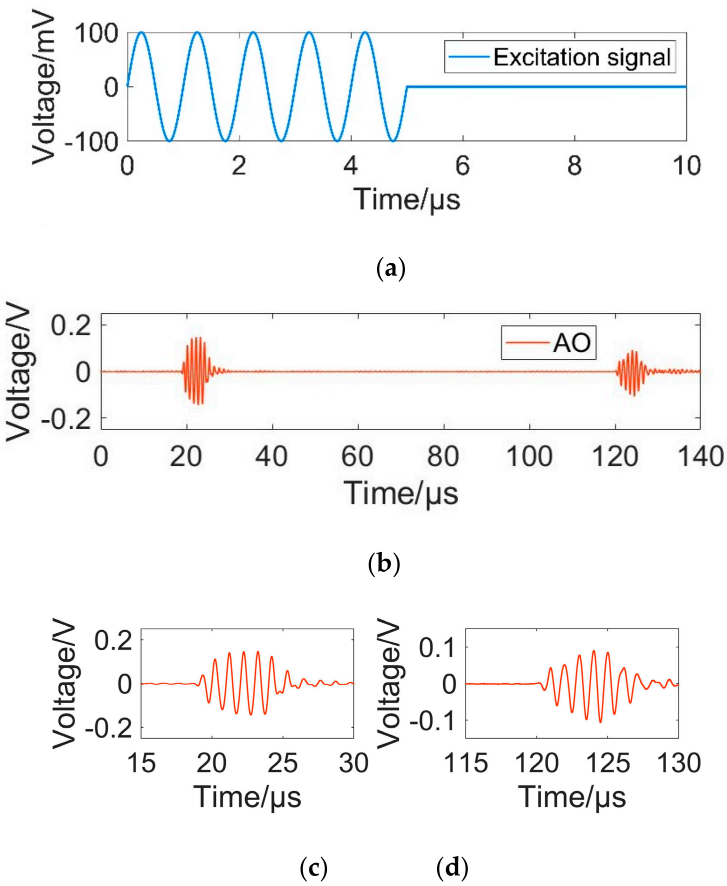

Figure 6. Ultrasound excited by sinusoidal burst signal: (**a**) 5-cycle 1 MHz burst signal; (**b**) ultrasound signal detected by laser sensing system; (**c**,**d**) zooms of the signal.

5. Results and Discussion

5.1. TOF by the Cross-Correlation Method

The reference signal is the signal that is transmitted by the transducer and first passes through the laser beam. The echo wave is the wave that is reflected from the target. The cross-correlation coefficient is calculated at each point of the ultrasound signal. The laser sensing system makes it possible to record both the reference signal and echoes without disturbing the ultrasound. Please note that they are all recordings of the same ultrasound pulse at different times. Although the ultrasound propagates in the opposite direction after it is reflected, the signal series recorded by the laser do not need to be reversed, as shown in Figure 6.

The reference signal is Ref(t), and the echoes are $S(t)$ as follows:

$$S(t) = \sum a_i \mathrm{Ref}(t - \tau_i), \tag{10}$$

where i is the ith echo, a_i is the reflection coefficient and τ_i is the time delay of the echo to the reference signal. Usually, we consider the first echo as the signal reflected from the target. The cross-correlation coefficient $C(\tau)$ is calculated by Equation 8, and the result is shown in Figure 7b. The envelope of the cross-correlation coefficient is calculated by the Hilbert transform. The first peak of the envelope refers to the moment that the ultrasound propagates through the laser light, which is the starting point of TOF. The TOF is defined as the duration t between peaks. The distance is the distance between the reference plane and the reflected plane, as shown in Figure 3. Although the TOF can be calculated by the envelope of the ultrasound signal, which is shown in Figure 7c, the signal distortion would cause error and distortion. Compared to Figure 7c, the envelope of the cross-correlation coefficient shows better smoothness and symmetry. With a stable and clean reference signal, an accurate TOF can be calculated according to the cross-correlation method. A plane wave is emitted by the transducer. At each test point, the ultrasound can be seen as propagating along a straight line.

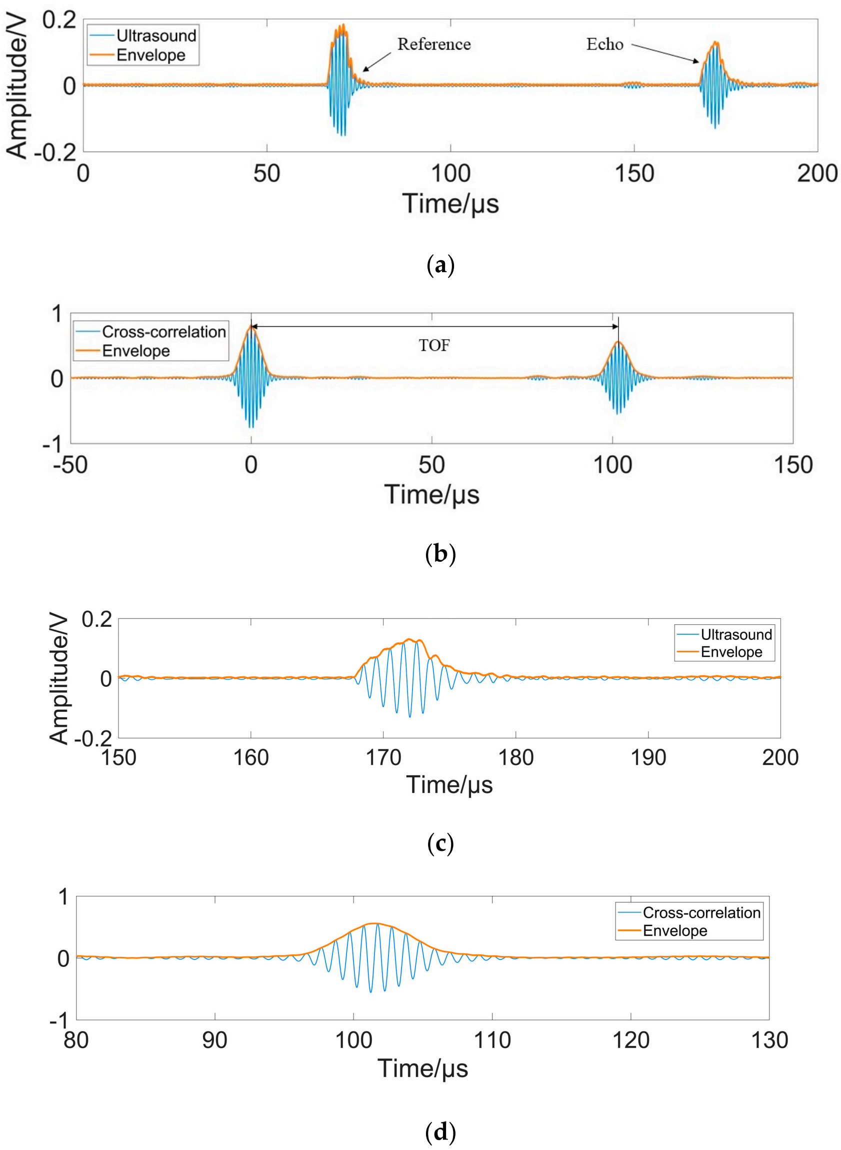

Figure 7. (**a**) The reference signal and echo wave in the ultrasound signal; (**b**) the cross-correlation coefficient and envelope of the ultrasound; (**c**) zooms of (**a**); (**d**) zooms of (**b**).

There are some factors that impact on the performance of the proposed method. First, the sampling rate determines the time resolution of the cross-correlation method. However, a high sampling rate leads to expensive equipment and large data sizes. In this experiment, the sampling rate is 1 GHz, and we interpolate it to 2.5 GHz using linear interpolation. Interpolation is commonly used in cross-correlation calculations to improve the measurement resolution, without affecting the accuracy [43,44]. The time resolution is 0.4 ns, in theory. Second, stochastic noise is the main noise in the proposed method. Two ways to reduce stochastic noise in the experiment are bandwidth limitation and average sampling. The central frequency of the transducer is 1 MHz. As such, the limiting frequency of the filter is set at 20 MHz. Eight average times are suitable in this experiment, considering both the SNR and time consumption. In addition, pulse repetition frequency (PRF) here is 200 Hz. On one hand, the PRF determines the maximum ranging distance, which is 3.75 m when the sound velocity is 1500 m/s. On the other hand, at each measurement point, the detection signal is the mean of eight sampling results. Thus, the PRF should not be too small.

Although the positions of the transducer and laser were fixed, temperature variation, vibration, and electrical noise would cause a shift in the signal. The repeatability of the TOF measurements in 50 continuous tests at distances of 30 cm and 80 cm is shown in Figure 8. Both were less than 4 ns at a distance up to 80 cm.

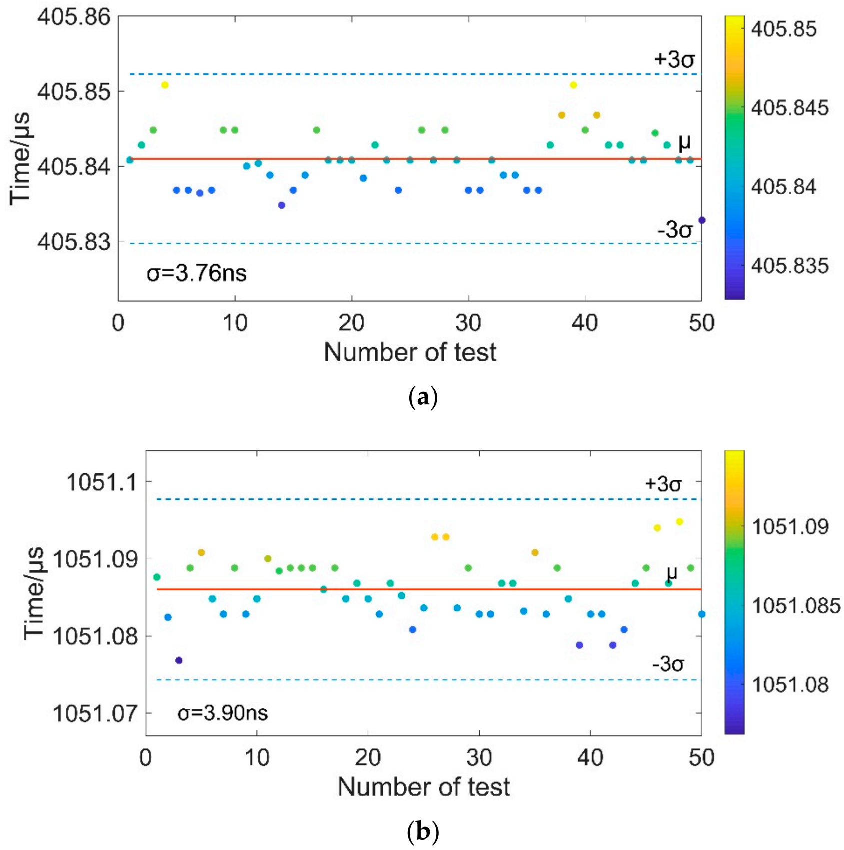

Figure 8. The repeatability of TOF measurements in 50 continuous tests: (**a**) At a distance of 30 cm; (**b**) at a distance of 80 cm.

5.2. Sound Velocity

The sound velocity was measured by a mini SVP from Valeport. It was fitted with a digital TOF sound velocity sensor, a temperature sensor, and strain gauge pressure transducer. The resolution of sound velocity is 0.001 m/s, and the uncertainty of sound velocity is 0.02 m/s. The sound velocity was measured after the temperature remained stable. The sound velocity measured for different places in the water tank is shown in Figure 9. The repeatability error of sound velocity was less than 0.003 m/s. The error of sound velocity at different places was less than 5×10^{-4} m/s.

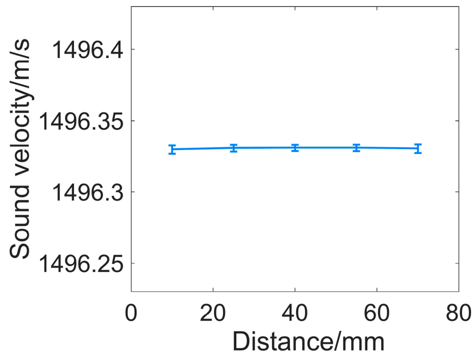

Figure 9. Sound velocity measured at different places in the water tank.

5.3. Ranging Resolution

In conventional ultrasound ranging techniques, the ranging resolution is equal to the half-wavelength of the wave. Unlike amplitude-based ranging methods, phase-based ranging methods, such as the cross-correlation method used in this paper, can improve the ranging resolution to subwavelength. The time resolution is 0.4 ns in theory, and the theoretical ranging resolution can achieve 1 μm.

In this situation, the target was fixed on the displacement platform. The ranging results by conventional ultrasonic ranging and the proposed system with a step distance of 0.05 mm are shown in Figure 10. At each measuring point, we measured 10 times repeatedly. The deviation of ultrasonic ranging was larger than the proposed method.

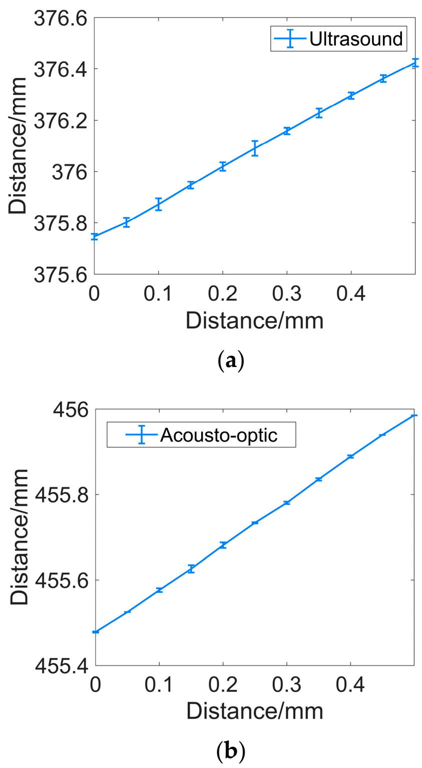

Figure 10. Ranging results with a step distance of 0.05 mm: (**a**) Ultrasonic ranging; (**b**) the proposed ranging.

The ranging results from the proposed system with a step distance of 0.01 mm are shown in Figure 11. The deviation was less than 0.004 mm, and the linearity was good. The ranging resolution could reach at least 0.01 mm in practice.

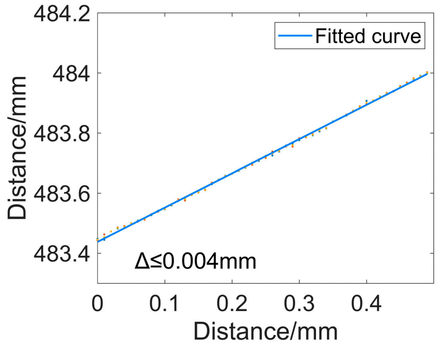

Figure 11. Ranging results with a step distance of 0.01 mm.

5.4. Ranging Results

The distance of each target was measured by a coordinate measuring machine, which was viewed as the reference distance. The coordinate measuring machine was a Global Classic SR07.10.07 from Hexagon. The measuring error in space is less than 1.9 μm. The positioning repeatability is less than 5 μm. For each target, we measured the spatial position of 12 points and fitted a plane. The distance of each target was calculated by all the measuring points.

The ranging results of the five targets using the laser sensing system and cross-correlation method are shown in Figure 12. For each target, we took 10 repeated measurements. The average values are shown in Figure 12. The ultrasonic transducer used here was the 1P28.

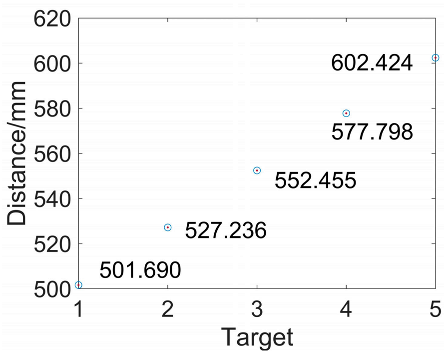

Figure 12. The ranging results of the five targets using the proposed method.

A comparison of the results for the coordinate measuring machine and the proposed method is shown in Table 2. We use the distance variations measured by our system to compare to values measured by the coordinate measuring machine. The accuracy was better than 0.3 mm. The average relative error was nearly less than 1% for all targets. The proposed method showed good accuracy compared to the coordinate measuring machine.

Table 2. Comparison of ranging results.

Target	Results by the Coordinate Measuring Machine/mm	Results by the Proposed Method /mm	Relative Error
1–2	25.351	25.545	0.77%
2–3	25.033	25.219	0.74%
3–4	25.174	25.343	0.67%
4–5	24.602	24.439	−0.66%
1–3	50.496	50.764	0.53%
1–4	75.858	76.108	0.33%
1–5	100.447	100.734	0.29%

5.5. Thickness Detection Results

The test piece was an aluminum block, which is shown in Figure 13. The two sides of the test piece could be viewed as 17 mm high steps. One side of the test piece was covered with a piece of paper and tape. Please note that the ultrasonic transducer used here was the 1P20. The test piece was placed at the bottom of the water tank. The transducer was placed on the surface of the test piece at a distance of 15 cm. Therefore, the direction of ultrasound propagation was along the *x*-axis, which is shown in Figure 14. The thickness of the aluminum block is calculated by the range difference of the surface of the aluminum block and the subsurface of the water tank.

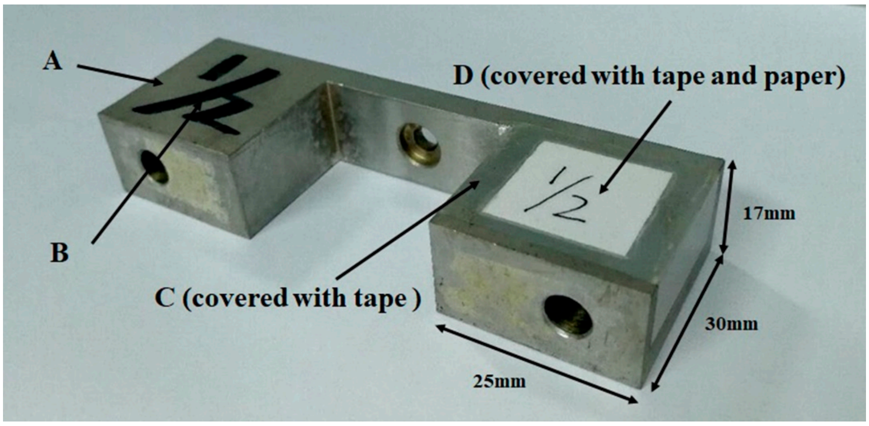

Figure 13. Image of the test piece and measuring points.

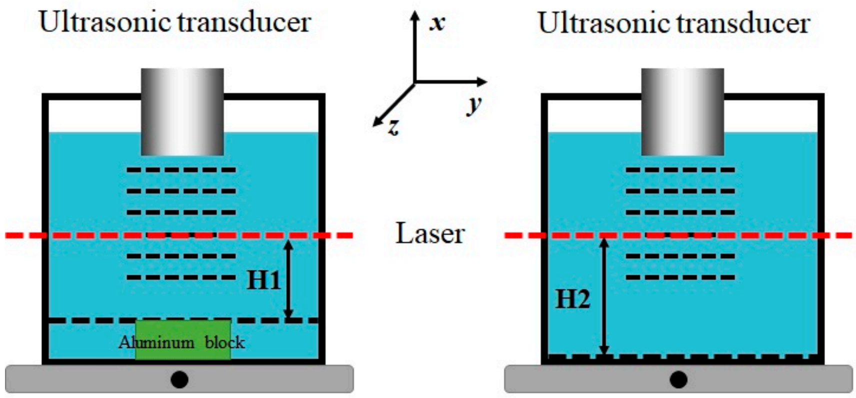

Figure 14. Measurement of the thickness of the aluminum block; the thickness is the difference between H1 and H2.

The thickness of the test piece was measured using the micrometer. Four different points of the test piece were measured, as shown in Figure 13. The results are listed in Table 3. The model of micrometer used was a Micromar 40 ER, with a resolution of 0.001 mm. The main measuring error was due to the measurement mode. The proposed ranging system was a noncontact measurement method. The height of the test piece was calculated by the range difference of the surface of the test piece and the subsurface of the water tank, whereas the micrometer was a contact measurement. The relative error was less than 1.3%.

Table 3. Measurement results of the test piece.

Measurement Point	Results/mm	Results by Micrometer/mm	Relative Error
A	17.158	16.983	1.03%
B	17.181	16.977	1.20%
C	17.222	17.022	1.17%
D	17.303	17.102	1.17%

5.6. Uncertainty Analysis

The distance calculated by pulse-echo system is calculated by the following:

$$s = \frac{1}{2}vt. \tag{11}$$

Therefore, the measurement uncertainty of the distance of the targets in this experiment can be calculated as follows:

$$u^2(s_m) = [\frac{\partial s}{\partial v}u(v_{measured})]^2 + [\frac{\partial s}{\partial t}u(t_{measured})]^2 + [u(s_{expansion})]^2 + [u(s_{measured})]^2. \tag{12}$$

The uncertainty of sound velocity is $u(v_{measured})$, which is a combination of three uncertainty sources. The accuracy of sound velocity measured by the mini SVP, $v_{accuracy}$, is 0.02 m/s. The repeatability error of sound velocity, $v_{repeatability}$, is 0.003 m/s. The uniformity of sound velocity in the water tank is 5×10^{-4} m/s. Therefore, the $u(v_{measured})$ is 2.35×10^{-2} m/s.

The uncertainty of TOF is $u(t_{measured})$. The main component is the repeatability error of TOF, $t_{repeatability}$, which is 4.0 ns.

The uncertainty of the measured value of the distance is $u(s_{measured})$. It is the maximum of standard deviation compared to the reference distance, which is 0.199 mm. Uncertainty of the thermal expansion coefficient, $u(s_{expansion})$, is $1.18 \times 10^{-6} \times T \times s_m$. The temperature variation T is 0.05 K. However, if the distance is not too long, it can be neglected.

The uncertainty sources are shown in Table 4. We use the distance of target 1–2 as an example. In summary, the combined uncertainty of the proposed ranging system can be estimated as follows:

$$u^2(s_m) = (v_{measured} \cdot 4.0\ \text{ns})^2 + (t_{measured} \cdot 11.75\ \text{mm/s})^2 + (1.9\ \mu\text{m} + 3.3 \times 10^{-3} \cdot s_m)^2 + (0.1990\ \text{mm})^2. \tag{13}$$

Table 4. Uncertainly analysis of the proposed ultrasonic ranging system.

Standard Uncertainty Component: $u(x_i)$	Source of Uncertainty	Uncertainty: $u(x_i)$	Uncertainty Value: $\mid c_i \mid u(x_i)$ Distance of Target 1–2
$u(t_{measured})$	Repeatability of TOF	4.0 ns	3×10^{-2} mm
$u(v_{measured})$	Uncertainty of sound velocity	2.35×10^{-2} m/s	0.013 mm
$u(v_{accuracy})$	Accuracy of the SVP	0.02 m/s	
$u(v_{repeatability})$	Repeatability of sound velocity	0.003 m/s	
$u(v_{uniformity})$	Uniformity of sound velocity in water tank	5×10^{-4} m/s	
$u(s_{measured})$	Uncertainty of the measured value of the distance	0.199 mm	0.199 mm
$u(s_{expansion})$	Uncertainty of the thermal expansion coefficient	$1.18 \times 10^{-6} \times T \times s_m$	4.7×10^{-5} mm
The combined uncertainty is calculated by the Equation (13). The combined value of the distance of target 1–2 is 0.202 mm.			

6. Conclusions and Future Work

In this paper, we design a high-resolution ultrasonic ranging system using a laser sensing system and the cross-correlation method. The laser sensing system is a noncontact ultrasound detection technique based on acousto-optic diffraction, which shows high SNR compared to conventional ultrasonic transducers. It can record the ultrasound that is transmitted from the transducer as the reference signal without disturbing the ultrasound field. The stable and clean reference signal provides an accurate TOF calculated by the cross-correlation method. The time resolution is 0.4 ns, in theory. The repeatability error of TOF is less than 4 ns at a distance up to 0.8 m. The ranging resolution can reach 0.01 mm, which is less than one-tenth of the wavelength of ultrasound.

The ranging results of five targets are compared with the coordinate measuring machine. The accuracy is better than 0.3 mm and the relative error is less than 1%. The thickness detection result of the test piece is compared with the micrometer. The relative error is less than 1.3%. Even a piece of paper can be distinguished using the proposed method.

The proposed system shows potential for combining the laser sensing system with a conventional ultrasound detection method. In our future work, we will take advantage of the laser sensing system for potential applications in underwater ultrasonic ranging and underwater imaging.

Author Contributions: B.X. and S.C. designed the experiment. L.J. and H.W. performed the experiment. X.Y. and H.W. analyzed the data. L.J. wrote the original manuscript. J.Z. and Z.Z. did the review and editing.

Funding: This research was funded by the Major Scientific Instrument and Equipment Development Project in National Key Research and Development Program of China, grant numbers 2016YFC1401203 and 2016YFF0101802; the National Natural Science Foundation of China, grant number 61505140; the Natural Science Foundation of Tianjin, grant number 18JCYBJC17100; and Research projects of Tianjin Municipal Education Commission, grant number JWK1616.

Acknowledgments: We thank Chenglin Wang for distance calibration of targets by the coordinate measuring machine. We thank Zhiyang Wang for his help in sound velocity measurement using mini SVP.

Conflicts of Interest: The authors declare no conflict of interest.

References

1. Jiang, S.B.; Yang, C.M.; Huang, R.S.; Fang, C.Y.; Yeh, T.L. An innovative ultrasonic time-of-flight measurement method using peak time sequences of different frequencies: Part I. *IEEE Trans. Instrum. Meas.* **2011**, *60*, 735–744. [CrossRef]
2. Wu, H.; Chen, J.; Wu, S.; Jin, H.; Yang, K. A model-based regularized inverse method for ultrasonic b-scan image reconstruction. *Meas. Sci. Technol.* **2015**, *26*, 628–634. [CrossRef]
3. Drinkwater, B.W.; Wilcox, P.D. Ultrasonic arrays for non-destructive evaluation: A review. *NDT E Int.* **2006**, *39*, 525–541. [CrossRef]
4. Nakahira, K.; Kodama, T.; Furuhashi, T.; Okuma, S. A self-adapting sonar ranging system based on digital polarity correlators. *Meas. Sci. Technol.* **2004**, *15*, 347. [CrossRef]
5. Jin, H.; Wu, E.; Han, Y.; Yang, K.; Chen, J. Frequency domain synthetic aperture focusing technique for variable-diameter cylindrical components. *J. Acoust. Soc. Am.* **2017**, *142*, 1554–1562. [CrossRef] [PubMed]
6. Zhao, J.; Gaydecki, P.A.; Burdekin, F.M. A numerical model of ultrasonic scattering by a defect in an immersion test. *Ultrasonics* **1995**, *33*, 271–276. [CrossRef]
7. Olofsson, T. Phase shift migration for imaging layered objects and objects immersed in water. *IEEE Trans. Ultrason. Ferroelectr. Freq. Control* **2010**, *57*, 2522–2530. [CrossRef]
8. Wu, J.; Zhu, J.; Yang, L.; Shen, M.; Xue, B.; Liu, Z. A highly accurate ultrasonic ranging method based on onset extraction and phase shift detection. *Measurement* **2014**, *47*, 433–441. [CrossRef]
9. Hasan, R.; Ierodiaconou, D.; Monk, J. Evaluation of four supervised learning methods for benthic habitat mapping using backscatter from multi-beam sonar. *Remote Sens.* **2012**, *4*, 3427–3443. [CrossRef]
10. Foo, K.Y.; Atkins, P.R.; Collins, T. Sea trials of bi-static time-domain incoherent synthetic aperture sonar. *Electron. Lett.* **2004**, *40*, 341–343. [CrossRef]
11. Barshan, B. Fast processing techniques for accurate ultrasonic range measurements. *Meas. Sci. Technol.* **2000**, *11*, 45–50. [CrossRef]
12. Queiros, R.; Alegria, F.C.; Girao, P.S.; Serra, A.C. Cross-correlation and sine-fitting techniques for high-resolution ultrasonic ranging. *IEEE Trans. Instrum. Meas.* **2010**, *59*, 3227–3236. [CrossRef]
13. Huang, C.F.; Young, M.S.; Li, Y.C. Multiple-frequency continuous wave ultrasonic system for accurate distance measurement. *Rev. Sci. Instrum.* **1999**, *70*, 1452–1458. [CrossRef]
14. Huang, K.N.; Huang, Y.P. Multiple-frequency ultrasonic distance measurement using direct digital frequency synthesizers. *Sens. Actuator A-Phys.* **2009**, *149*, 42–50. [CrossRef]
15. Figueroa, F.; Barbieri, E. An ultrasonic ranging system for structural vibration measurements. *IEEE Trans. Instrum. Meas.* **1991**, *40*, 764–769. [CrossRef]
16. Parrilla, M.; Anaya, J.J.; Fritsch, C. Digital signal processing techniques for high accuracy ultrasonic range measurements. *IEEE Trans. Instrum. Meas.* **1991**, *40*, 759–763. [CrossRef]
17. Angrisani, L.; Baccigalupi, A.; Moriello, R.S. A measurement method based on kalman filtering for ultrasonic time-of-flight estimation. *IEEE Trans. Instrum. Meas.* **2006**, *55*, 442–448. [CrossRef]

18. Marioli, D.; Narduzzi, C.; Offelli, C.; Petri, D.; Sardini, E.; Taroni, A. Digital time-of-flight measurement for ultrasonic sensors. *IEEE Trans. Instrum. Meas.* **1992**, *41*, 93–97. [CrossRef]
19. Gueuning, F.E.; Varlan, M.; Eugne, C.E.; Dupuis, P. Accurate distance measurement by an autonomous ultrasonic system combining time-of-flight and phase-shift methods. *IEEE Trans. Instrum. Meas.* **1997**, *46*, 1236–1240. [CrossRef]
20. Queirós, R.; Corrêa, A.; Francisco, S.P.; Cruz, S.A. A multi-frequency method for ultrasonic ranging. *Ultrasonics* **2015**, *63*, 86–93. [CrossRef] [PubMed]
21. Xue, B.; Wang, Z.; Zhang, L.; Wu, H. Absolute distance measurement using optical sampling by sweeping the repetition frequency. *Opt. Laser Eng.* **2018**, *109*, 1–6. [CrossRef]
22. Wu, H. Intensity evaluation using a femtosecond pulse laser for absolute distance measurement. *Appl. Opt.* **2015**, *54*, 5581–5590. [CrossRef] [PubMed]
23. Khyam, M.O.; Ge, S.S.; Xinde, L.; Pickering, M.R. Highly accurate time-of-flight measurement technique based on phase-correlation for ultrasonic ranging. *IEEE Sens. J.* **2017**, *17*, 434–443. [CrossRef]
24. Lashkari, B.; Zhang, K.; Dovlo, E.; Mandelis, A. Coded excitation waveform engineering for high frame rate synthetic aperture ultrasound imaging. *Ultrasonics* **2017**, *77*, 121–132. [CrossRef]
25. Qiu, Y.; Gigliotti, J.V.; Wallace, M.; Griggio, F.; Demore, C.E.M.; Cochran, S.; Trolier-McKinstry, S. Piezoelectric micromachined ultrasound transducer (PMUT) arrays for integrated sensing actuation and imaging. *Sensors* **2015**, *15*, 8020–8041. [CrossRef]
26. Rolland, Q.; Oudich, M.; Eljallal, S.; Dupont, S.; Pennec, Y.; Gazalet, J.; Kastelik, J.C.; Leveque, G.; Djafari-Rouhani, B. Acousto-optic couplings in two-dimensional phoxonic crystal cavities. *Appl. Phys. Lett.* **2012**, *101*, 061109. [CrossRef]
27. Savage, N. Acousto-optic devices. *Nat. Photonics* **2010**, *4*, 728–729. [CrossRef]
28. Farmer, D.J.; Akimov, A.V.; Gippius, N.A.; Bailey, J.; Sharp, J.S.; Kent, A.J. High-frequency acousto-optic effects in Bragg reflectors. *Opt. Express* **2014**, *22*, 15218–15231. [CrossRef]
29. Kastelik, J.C.; Dupont, S.; Benaissa, H.; Pommeray, M. Bifrequency acousto-optic beam splitter. *Rev. Sci. Instrum.* **2006**, *77*, 075103. [CrossRef]
30. Scott, M.L.; Jernigan, J.; Hutcheson, L.; Gould, D. Fast acousto-optic lens Q switch. *J. Appl. Phys.* **1975**, *46*, 3483–3488. [CrossRef]
31. Raman, C.V.; Nath, N.S.N. The diffraction of light by high frequency and sound waves: Part 1. *Proc. Indian Acad. Sci.* **1936**, *2*, 406–412. [CrossRef]
32. Klein, W.R.; Cook, B.D. Unified approach to ultrasonic light diffraction. *IEEE Trans. Sonics Ultrason.* **1967**, *14*, 123–134. [CrossRef]
33. Abeele, K.V.D.; Leroy, O. Light diffraction by ultrasonic pulses: Analytical and numerical solutions of the extended Raman–Nath equations. *J. Acoust. Soc. Am.* **1990**, *88*, 2298–2315. [CrossRef]
34. Jiang, X.; Cheng, Q.; Xu, Z.; Qian, M.; Han, Q. Quantitative measurement of acoustic pressure in the focal zone of acoustic lens-line focusing using the schlieren method. *Appl. Opt.* **2016**, *55*, 2478–2483. [CrossRef]
35. Pulkkinen, A.; Leskinen, J.J.; Tiihonen, A. Ultrasound field characterization using synthetic schlieren tomography. *J. Acoust. Soc. Am.* **2017**, *141*, 4600–4609. [CrossRef]
36. Pitts, T.A.; Sagers, A.; Greenleaf, J.F. Optical phase contrast measurement of ultrasonic fields. *IEEE Trans. Ultrason. Ferroelectr. Freq. Control* **2001**, *48*, 1686–1694. [CrossRef]
37. Reibold, R.; Kwiek, P. Uncertainty considerations of ultrasonic field mapping by light-diffraction tomograph. *Ultrasonics* **1997**, *35*, 187–193. [CrossRef]
38. He, L.; Zhu, F.; Chen, Y.; Duan, K.; Lin, X.; Pan, Y. Ultrasonic power measurement system based on acousto-optic interaction. *Rev. Sci. Instrum.* **2016**, *87*, 054903. [CrossRef]
39. Almqvist, M.; Holm, A.; Persson, H.W.; Lindström, K. Characterization of air-coupled ultrasound transducers in the frequency range 40 kHz-2 MHz using light diffraction tomography. *Ultrasonics* **2000**, *37*, 565–575. [CrossRef]
40. Feldman, M. Hilbert transform in vibration analysis. *Mech. Syst. Signal Process.* **2011**, *25*, 735–802. [CrossRef]
41. Fisher, B.T.; Hahn, D.W. Real-time measurement of ArF excimer laser corneal tissue ablation rates using cross-correlation of laser waveforms. *Opt. Express* **2011**, *19*, 4231–4241. [CrossRef] [PubMed]
42. Jia, L.; Xue, B.; Chen, S.; Wu, H.; Yang, X.; Zhai, J.; Zeng, Z. Characterization of pulsed ultrasound using optical detection in Raman-Nath regime. *Rev. Sci. Instrum.* **2018**, *89*, 084906. [CrossRef] [PubMed]

43. Lai, X.; Torp, H. Interpolation methods for time-delay estimation using cross-correlation method for blood velocity measurement. *IEEE Trans. Ultrason. Ferroelectr. Freq. Control* **1999**, *46*, 277–290. [PubMed]
44. Costa-Júnior, J.F.S.; Cortela, G.A.; Maggi, L.E.; Rocha, T.F.D.; Pereira, W.C.A.; Costa-Felix, R.P.B. Measuring uncertainty of ultrasonic longitudinal phase velocity estimation using different time-delay estimation methods based on cross-correlation: Computational simulation and experiments. *Measurement* **2018**, *122*, 45–56. [CrossRef]